Microstructure imaging of Florentine stuccoes through X-ray tomography: A new insight on ancient plaster-making techniques

Florian Beaugnon, Gianluca Gariani, Emmanuelle Gouillart, Anne Bouquillon, Marc Bormand, Gilles Wallez

Microstructure imaging of Florentine stuccoes through x-Ray tomography: a new insight on ancient plaster-making techniques

Authors:
Florian BEAUGNON [a,b,c]
Gianluca GARIANI [a,b,d,e]
Emmanuelle GOUILLART [c]
Anne BOUQUILLON [a,b]
Marc BORMAND [f]
Gilles WALLEZ [a,b,g]

Authors affiliations:
a Centre de Recherche et de Restauration des Musées de France (C2RMF), Ministère de la Culture et de la Communication, 14, quai François-Mitterrand, 75001 Paris, France
b Chimie ParisTech, PSL Research University, CNRS, Institut de Recherche Chimie Paris (IRCP), 75005 Paris, France
c Joint Unit CNRS/Saint-Gobain, Surface du Verre et Interfaces (SVI), 39 quai Lucien Lefranc 93303 Aubervilliers, France
d Laboratoire de Physicochimie des Polymères et des Interfaces (LPPI), Université de Cergy-Pontoise, 5, mail Gay-Lussac, Neuville-sur-Oise, 95031 Cergy-Pontoise cedex, France
e Fondation des Sciences du Patrimoine, LabEX PATRIMA, 33, boulevard du Port, MIR de Neuville, 95011 Cergy-Pontoise, France
f Musée du Louvre, 75001 Paris, France
g UFR 926, Sorbonne Université, 75005 Paris, France

Abstract:
Gypsum-based plasters or stuccoes, in spite of their importance and diffusion, received little attention in cultural heritage materials studies. This work introduces a new, non-destructive methodology, using micro-tomography to measure the water/plaster ratio and the morphology of the hemihydrate powder used to make plasters on < 1mm^3 samples. This methodology give insight in both the raw material (and ultimately provenance) and the technique used to make plaster.
The methodology was tested first on mock-up samples of known composition, then in a case study on 13 low-relief cast plaster sculptures from 15th century Florentine artists.
Preliminary conclusions on this limited corpus show relative uniformity across most reliefs in terms of raw materials and techniques. The casts of one model (Nativity, attributed to Donatello and B. Bellano) were made with a different raw material, in line with prior geochemical analyses ; these results support the previous attribution to a North Italian rather than Florentine origin. The casts of a second model (Virgin and Child, type of Saint Petersburg, attributed to Antonio Rossellino) were prepared with a different technique. This surprising result was not expected from Art History or previous studies.

Keywords:
Gypsum; Plasters; Renaissance stuccoes; X-Ray microtomography; Porosity

Highlights:
New method for the study of ancient gypsum plasters
Characterisation of porosity using microtomography
Inedite microstructural study of 13 Florentine stuccoes

1. Introduction

Gypsum ($CaSO_4\text{-}2H_2O$), formed as an evaporite mineral, is the raw material used in the manufacture of plasters. When heated above 100-120 °C [1] it releases part of its water as vapor and forms calcium sulfate hemihydrate, the main constituent of the reactive plaster powder (eq. 1).

$$CaSO_4 \cdot 2H_2O \rightarrow CaSO_4 \cdot 0.5H_2O + 1.5H_2O(g) \quad (1)$$

Mixed with water in a slurry, hemihydrate dissolves and recrystallises to set as secondary gypsum crystals (eq. 2).

$$CaSO_4 \cdot 0.5H_2O + 1.5H_2O(l) \rightarrow CaSO_4 \cdot 2H_2O \quad (2)$$

Other phases can appear during or after the calcination of primary gypsum: when exposed to a wet atmosphere, hemihydrate turns to $CaSO_4\text{-}0.625H_2O$ [2]; soluble anhydrite (γ-$CaSO_4$) forms if the calcination is run in a dry atmosphere or at a slightly higher temperature [1]. Both these soluble subhydrates behave like hemihydrate when mixed with water. However, at higher temperatures of 250-350 °C, γ-anhydrite transforms into insoluble anhydrite (β-$CaSO_4$) [3]. This unreactive phase behaves as a charge that does not take part in the setting, thus lowering the mechanical properties of the final material. For these reasons, the β-$CaSO_4$ is generally unwanted and is only present as a result of excessive heating or from impurities in the raw gypsum.

The setting of the plaster is a two-step process. The dissolution of hemihydrate grains is quickly halted by the saturation of the solution, and gypsum seeds slowly appear during an activation period of several minutes. In a second step, the growth of the gypsum crystals depletes the solution and the hemihydrate grains are completely dissolved [4].

As for any hydraulic binder, the proportion of water and hemihydrate is an important parameter as it affects the rheology of the slurry and the density of the final material. It is quantified through the water-to-plaster ratio (W/P), based on the masses of the ingredients mixed to make the slurry. As only a small amount of water takes part in the re-hydration reaction (eq. (2)), most of it is left at the end of the reaction.

Pores can be observed at several scales after drying. Macropores (typical size of a few hundreds of microns up to several millimeters in diameter) result from the trapping of air bubbles. The excess water that dries off leaves pores in the plaster at two additional scales : micropores of small size (under 10 μm) are found between crystals of secondary gypsum. Finally, the two-step reaction leads to the formation of mesopores (ranging in size from a few dozens to a few hundreds of microns). Their morphology results from the chronology of the setting of plaster, as secondary gypsum grows from seeds that form outside of hemihydrate grains, leaving "ghost pores" of identical shape after their dissolution (fig. 1) [5].
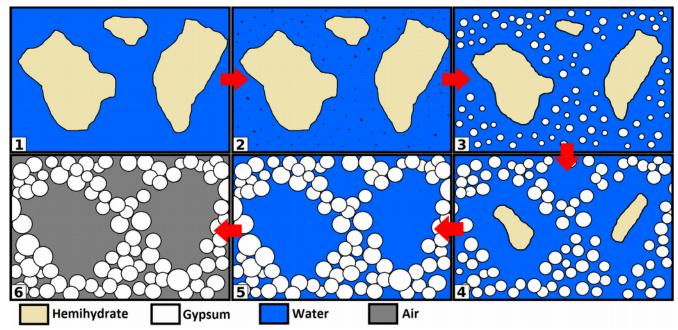
Figure 1 : Setting of plaster. *The dissolution of hemihydrate and growth of gypsum is a two-step process: at first, gypsum seeds appear in the saturated solution with no significant dissolution of hemihydrate grains (1-2); gypsum crystals then grow while hemihydrate grains are dissolved until the reaction is complete (3-5). Excess water then dries off leaving pores behind (6). Drawn after J. Adrien et al. [5].*

Both the total porosity and the morphology of the mesopores are of interest for the study of ancient plasters. The total porosity can be used to asses the W/P ratio. This ratio is adjusted depending on the casting technique, additives and intended use of the plaster. This makes it an important indicator of workshop practices. The morphology of the mesopores depends on the microstructures of the plaster powder; they are in turn affected by the crystal habitus of the primary gypsum and processing [5]. The morphology of the mesopores can thus be an indicator of the raw gypsum's crystal morphology and its transformation into a plaster powder.

Mercury intrusion porosimetry (MIP) is the go-to technique for the measurement of porosity in mineral materials, but can not be used with precious cultural heritage samples. The drying of the material prior to the measurement (common methods involve oven-, freeze-, or solvent-drying [6]) as well as the trapping of mercury make it a destructive technique. This is often not acceptable with cultural heritage samples.
In addition, while MIP provides a measurement of the total porosity and the distribution of pores size, it is only sensitive to the open, interconnected porosity. Bottlenecks in pores also result in an in-/extrusion hysteresis that only allows to measure the smallest section. X-ray tomography has been proposed as a better alternative for the study of porous rocks [7] as it is not subject to these limitations. It also allows the additional characterisation of the pores' shape in three dimensions whith no damage to the sample, unlike the more traditional micrography on thin sections.
Tomography is routinely used for the characterisation of inorganic building materials, including gypsum plasters [8,9,10,11]. It has also been applied to various cultural heritage topics. However, its application to the characterisation of ancient gypsum plasters has only been attempted from the angle of macrostructures [12,13] and not from material sciences on a microscopic scale.

1.1 Research aims

This article reports on an exploratory work in which we researched a novel methodology for the analysis of ancient gypsum plasters, through a case study on samples taken from 15th century Florentine reliefs. This effort was motivated by the need to find non-destructive protocols to extract information on both the raw material and workshop practices of the past. In this contribution, we adress two questions:

1. Is it possible to measure the W/P ratio and the morphology of the reactive powder used to make plaster, on the basis of synchrotron X-ray microtomography data? Can this method be validated with mock-up samples of small (1 mm^3) size, as required for the characterisation of valuable works of Art?

2. Are these analysis useful for the study of ancient plasters, i.e. do they allow a meaningful comparison on a test corpus of a dozen sampled reliefs from the Renaissance and do they bring new insights in the study of these reliefs?

2. Materials

2.1 Historical artworks

13 cast plaster low-reliefs from the 15th century were sampled (fig. 2, table 1). They are part of a large production of artworks depicting religious scenes - almost exclusively compositions of the Virgin and Child - that were intended to be used as supports of private devotions in the homes of wealthy families [14]. They were originally painted, gilded and framed in wood or plaster. Some of the original models survive as marble, terracotta or bronze sculptures from which the plaster casts were most likely moulded [15,16].

The reliefs, cast in gypsum-based plaster (often described using the more generic "stucco" in artistic litterature), were manufactured in multiples after models by Florentine artists such as Lorenzo Ghiberti, Donatello, Luca Della Robbia, Antonio Rossellino, Desiderio da Settignano or Mino da Fiesole. While these artists spent most of their working life in Florence, some are known to have been active in other cities [17]. The original reliefs are expected to have been produced in the *bottegha* of the masters but might have been replicated in other workshops on the models they supplied. In addition, there is a possibility they were imitated in other places and at a later time. This is especially true for the 19th century when a resurgence of interest from collectors and academies could have prompted the making of forgeries [16, 18].

Figure 2: historical reliefs sampled. *From left to right : Nativity, 77x79 cm (RF 1191), Virgin and Child, type Pazzi, 68x52 cm (Inv. 242), Virgin and Child, type of the Candelabra, 78x52 cm (Camp. 20), Virgin and Child, type Saint Petersburg, 82x51 cm (Camp. 24). (c) C2RMF / J.-Y. Lacôte.*

Table 1 : historical reliefs sampled. *Inventory numbers, models and attributed authorship and cities of production of the models.*

Attribution (after/workshop of)	Model	Production centre	Inventory number
Donatello (Florence, 1378-1455)	Nativity	Northern Italy (Padua?)	RF 1191
Donatello	Nativity	Northern Italy (Padua?)	D 488
Donatello	Virgin and Child, Pazzi type	Florence	Inv 242
Luca della Robbia (Florence, 1399/1400-1482)	Virgin and Child, Massimo type	Florence	Inv 247
Desiderio da Settignano (Settignao, 1430 - Florence, 1464)	Virgin and Child, Turin type	Florence	RF 897
Antonio Rossellino (Settignano, 1427/1428-Florence, 1479)	Virgin and Child, Vienna type	Florence	Camp 16
Antonio Rossellino	Virgin and Child, Madonna of the Candelabra type	Florence	Camp 20
Antonio Rossellino	Virgin and Child, Madonna of the Candelabra type	Florence	1937-4
Antonio Rossellino	Virgin and Child, Madonna of the Candelabra type	Florence	DS 534
Antonio Rossellino	Virgin and Child, Madonna of the Candelabra type	Florence	MBA 587
Antonio Rossellino	Virgin and Child, Santa Maria Nova type	Florence	Inv 362
Antonio Rossellino	Virgin and Child, Saint Petersburg type	Florence	1937-3
Antonio Rossellino	Virgin and Child, Saint Petersburg type	Florence	Camp 24

This work is part of a larger project that aims at understanding the manufacturing techniques and sourcing of the raw material of these low-relief sculptures, including studies of the geology and chemistry of the binder [19] and of organic additives [20].

2.2 Recreation samples

In order to test the proposed methodology, mock-up samples were prepared with different hemihydrate powders (industrial vs. hand made). These were used for comparison of the mesopores morphologies; some were also prepared with different W/P ratio for the calibration of W/P measurements.

Three samples were made from hemihydrate plaster (plaster 1) supplied by Saint-Gobain Research Paris. They were each prepared from 100 g of plaster powder and W/P = 0.50, 0.70 and 1.00. The plaster powders and water were mixed for 30 seconds in a plastic cup where they were left to set.

A fourth mix of plaster was made starting with acicular crystals of gypsum heated at 120 °C for 6 h in a muffle furnace. The calcined plaster (plaster 2) was then ground up to a powder using a mortar and pestle and mixed with water at W/P = 0.6. The plaster powder was again mixed for 30 s in a plastic cup and left to set; two samples were analysed to check the repetability of measurements.

No additives are included in either plaster 1 or plaster 2. Nethertheless, naturally occuring impurites were searched for using quantitative Rietveld phase analysis. None were detected in plaster 2, while $CaCO_3$ (3.0(8) % by mass) was found in plaster 1.

2.3 Samples preparation

The plaster samples, a few mm^3 in size, were taken using a surgical scalpel from the surface of both historic and recreation plasters. Historic samples were extracted from the back and sides of the reliefs in places hidden to comply with deontological concerns.

To fit the 1.2 mm X-ray beam size, a 1 mm internal diameter polyimide tubing transparent to X-Rays was used as a sample holder. Most samples (both historical and recreations) were wider than 1 mm and broken into up to five fragments to fit inside the sample holder tubing. All of them were analyzed for a better measurement statistics.

3. Methods
3.1 Images acquistion

Our experiments were done on the ESRF synchrotron micro-tomography beamline ID19 [21,22]. The choice of the source was motivated by the intense, quasi-monochromatic pink-beam that only synchrotron radiation can provide. It is neccessary for an accurate measurement of the absorption coefficient regardless of the sample's thickness, in order to avoid beam hardening effects which are unavoidable with a polychromatic beam.

For each 3-D volume, 3000 radiographies were acquired over 180° with a sCMOS PCO Edge camera, corresponding to a pixel size of 0.65 micrometer and a scan time of two minutes. A 19.6 keV pink beam was used, and a 10 µm GGG scintillator converted the transmitted X-ray beam to visible light.

X-ray absorption maps were reconstructed in three dimensions from the raw data using the PyHST algorithm [23] and processed using the python package Scikit image [24,25] (fig. 3).
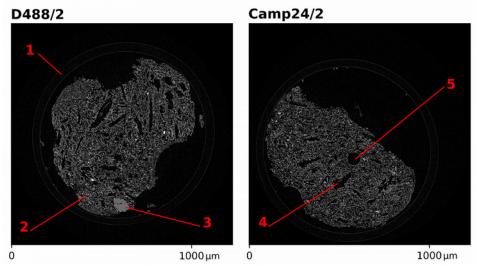

Figure 3: reconstructed X-Ray absorption images (slices). T*he samples can be seen inside sample holder tubes (1). In the secondary gypsum matrix (2) are primary gypsum inclusion (3) as well as pores. Mesopores (4) and trapped air bubbles (5) can be differentiated by the round shape of the latter.*

3.2 Measurement of water-to-plaster ratio
3.2.1 Calculations
The W/P ratio is defined as the mass of water m_W divided by the mass of plaster powder (hemihydrate) m_H mixed in the plaster slurry. After the reaction, the stoechiometric part of the water is structurally bound in the gypsum while the rest, left in excess, is liquid and fills the pores of the gypsum.

$$W/PR = \frac{m_W}{m_H} = \frac{m_{W,excess} + m_{W,gypsum}}{m_H} \quad (1)$$

The masses of structurally bound water and hemihydrate can be infered from the mass of gypsum in the set plaster and the molar masses of water, gypsum and hemihydrate (M_W, M_G, M_H):

$$W/PR = \frac{m_{W,excess} + \dfrac{1,5 M_W}{M_G} * m_G}{\dfrac{M_H}{M_G} * m_G} \quad (2)$$

The masses of water in excess and gypsum can be replaced in the formula by the multiplication of the respectives densities (d_W, d_G) and volumes; the volume occupied by excess water is equal to the measured porosity $V_{porosity}$ (3):

$$W/PR = \frac{d_W * V_{Porosity} + \dfrac{1,5 M_W}{M_G} * d_G * V_G}{\dfrac{M_H}{M_G} * d_G * V_G} \quad (3)$$

As it is a ratio, the volumes can be replaced by volumic fractions. Their sum is equal to one as the samples only contain gypsum and air, which mean that the W/P ratio can be expressed from the sole volumic fraction of gypsum v_G (4).

$$W/PR = \frac{d_W * (1 - v_G) + \dfrac{1,5 M_W}{M_G} * d_G * v_G}{\dfrac{M_H}{M_G} * d_G * v_G} \quad (4).$$

In addition, as X-ray absorption in air is negligible, the X-ray coefficient of linear absorption of the sample ρ_S only depends on v_G and the absorption coefficient of gypsum ρ_G: $\rho_S = v_G \rho_G$.

3.2.2 Image analysis
We segmented the samples from the background on the images using the absorption contrast between gypsum and air, with Otsu automated thresholding [26] and mathematical morphology operations such as dilation and /erosion filters features from Scikit-Image. The X-ray absorption coefficient was then averaged over the segmented sample volume.

3.2.3 Conditions for application
The W/P measurement relies on three assumptions :

1) The samples are only made up of secondary gypsum and air. Inclusion of materials with a different X-Ray absorption coefficient, such as mineral charges or unwanted β-$CaSO_4$. will skew the measurement of the total porosity. If impurities were present in significant amounts, corrections depending on their proportion and chemical nature would be neccessary.

2) The reactive plaster powder is pure hemihydrate ($CaSO_4$-$0.5H_2O$). Soluble anhydrite (γ-$CaSO_4$) or $CaSO_4$-$0.625H_2O$ are sometimes produced by the calcination of gypsum instead of hemihydrate. In plaster manufacture they will lead to slightly different results. However, they are not stable and quickly revert to hemihydrate when exposed to ambiant conditions of temperature and humidity [2,27].

3) There are no air bubbles. Air can be trapped in the slurry when mixing plaster powder and water. Unlike modern plasters that often include foaming agents though, ancient plasters typically show few bubbles that will not affect the measurement of W/P significantly.

3.2.4 Experimental validation

The X-ray linear absorption coefficient measured on recreation samples and plotted against the gypsum volumetric fraction (calculated in reverse from the known W/P) shows good linearity (fig. 4). The slope of the linear fit is found to be near the linear absorption coefficient of gypsum. ρ_G = 13.21 cm^{-1}, somewhat higher than the theoretical value of 11.31 cm^{-1} at an incident energy of 19.6 keV. Concievably, the difference results from the moderate energy dispersion of the incident beam.
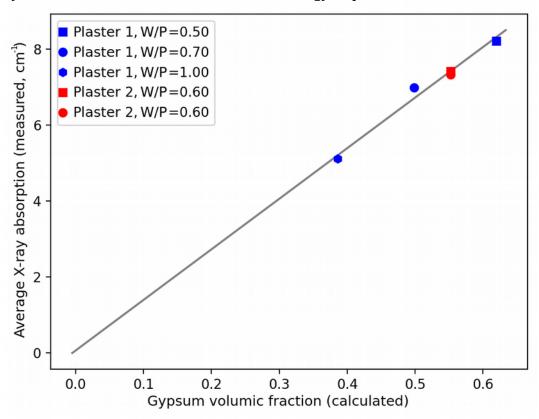

Figure 4: X-ray absorption and gypsum volumic fraction of recreation samples. *Measured average X-ray absorption coefficient vs calculated gypsum volumic fraction in recreation samples of known water-to-plaster ratio. The good linearity of our measurements can be seen with the regression line in black.*

The measurement of the W/P ratio proved to be reliable, with only limited deviation from calculated values. This deviation is acceptable considering the small size of the studied sample.

3.3 Measurement of pores size and morphology

3.3.1 Image analysis

Pores were segmented using Otsu's thresholding and dilation/erosion tools. An arbitrary lower cutoff of 10000 voxels was taken to make sure that only the significant mesopores were selected.

The sizes of the pores were recorded. Their irregular shapes (fig. 5) were approximated as ellipsoids of identical moment of inertia using Scikit image. The diameters $d_1 < d_2 < d_3$ of the ellipsoids were

divided to obtain aspect ratios $r_1 = d_1 / d_3$ and $r_2 = d_2 / d_3$ that describe the shape of the pores, independently of their size.

For each sample, we plotted both the normalized histogram of sizes and the unweighted average of aspect ratios r_1 and r_2.
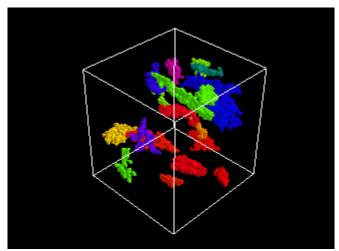

Figure 5: segmented pores. Three dimensional visualisation of segmented mesopores (grid cube 260 x 260 x 260 µm). The highly irregular shapes were approximated as ellipsoïds for comparison purposes.

3.3.2 Conditions for application
Only one assumption is neccesary for the measurement of pores morphology: the absence of trapped air bubbles. These are pores that will be measured accordingly, but their (spherical) shape is obviously not related to the morphology plaster powder. As seen in 3.2.3, trapped air bubbles are a rare occurence in ancient plaster samples.

3.3.3 Experimental validation
The measurement of pore size showed no significant difference in the distribution of sizes between the mock-up samples prepared with industrial plaster and those with plaster made in the lab using a mortar and pestle for grinding (fig 6). From this we can conclude that the distribution of pores sizes is not a relevant indicator of manufacturing processes.
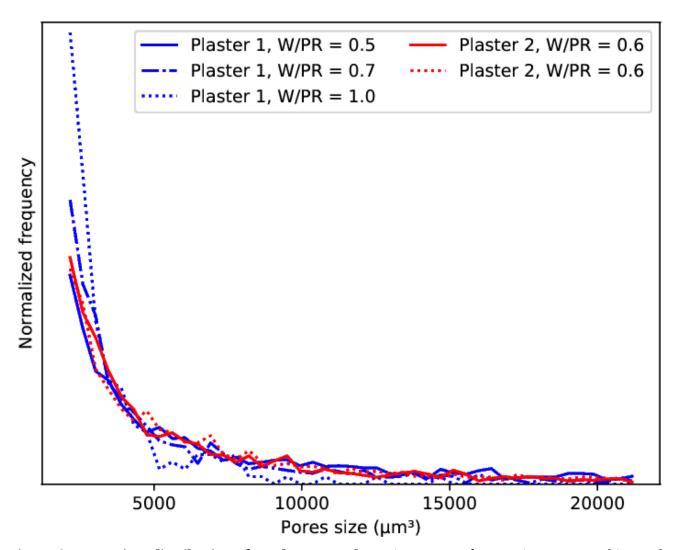
Figure 6: Pores sizes distribution of mock-up samples. *Histograms of pores sizes measured in mock-up samples, shown as a normalized frequency. Some variation is seen but is not correlated with the plaster powder used; it should rather be ascribed to statistical noise.*

The measurement of pores aspect ratios (fig. 7) was consistent across mock-up samples prepared with the same plaster powder while making a difference between those prepared with a different powder. In addition, the samples made from industrial plaster powder were prepared with different W/P and showed that the W/P ratio had no effect on the recorded pores shapes.
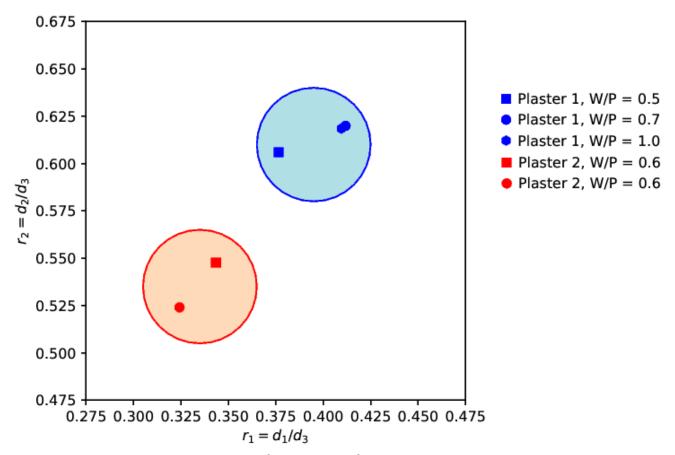
Figure 7: Averaged aspect ratios of the pores found in mock-up samples. *Averaged values computed from the aspect ratios of individual pores of historic samples. Cast made with industrial plaster 1 show higher aspect ratios $r_1 > 0.37$ and $r_2 < 0.60$ compared to $r_1 < 0.35$ and $r_2 < 0.55$ for plaster 2. Plaster 2 showing more elongated pores is consistent with the acicular habitus of the raw gypsum it was made from.*

4. Case study

In light of the results of Part 3, the W/P ratio as well as the average aspect ratios of pores were measured in historic samples, while the size distribution of the mesopores was not recorded. From these measurements an attempt was made to establish groups of artworks showing a material of similar W/P and pores shape, and to compare these groups with the models and historical backgrounds of the reliefs.

4.1 Results

4.1.1 Verification of the conditions of application

The chemical analysis of samples taken from the reliefs [19] shows that they are mainly made up of gypsum, even if the ratio between calcium and sulfate shows that there is a small fraction of calcium carbonate. Traces amounts of Na, Mg, Al, Si, P, Cl, K and Fe suggest the presence of dolomite, clays and halite in smaller amounts.

Bubbles due to trapped air are supposed to exhibit a roughly spherical shape. A quantitative assessment was made by counting those pores which exhibited aspect ratios higher than 0.9 (including bubbles but also regular shaped mesopores). Only faint amounts were found, ranging from 0 to 0.48% of all pores. This result is in agreement with the common opinion that ancient plasters were prepared without

foaming agents.

4.1.2 Water-to-plaster ratio

The results of the W/P measurement are shown in fig. 8. W/P ranged from 0.43 to 0.97. We observed a wide dispersion among fragments of the same sample with an overall standard deviation of 0.06 (and as high as 0.11 for individual relief Inv. 247).
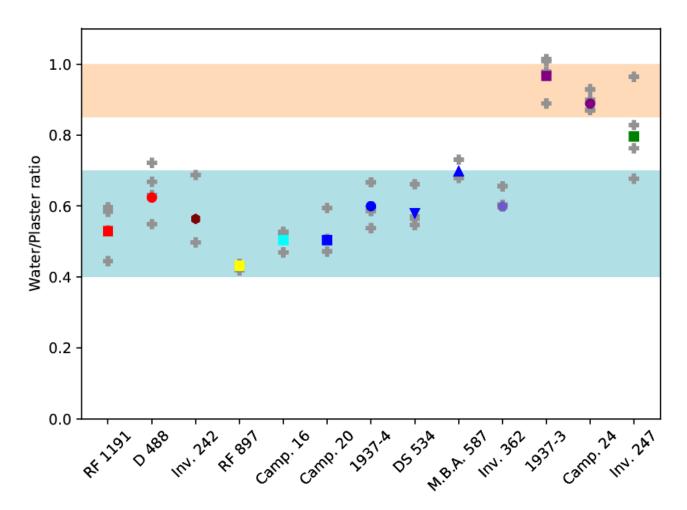

Figure 8 : Water-to-plaster ratio of historic samples. *Values for each fragment of sample are represented by grey crosses, the averaged W/P by colored markers. The ranges in blue and pink show the two main groups separated by their W/P: respectively the majority of the corpus (0.4 < W/P < 0.7) and the two reliefs of the Virgin and Child, type of St Petersburg (0.85 < W/P < 1). Relief Inv. 247 with its high dispersion overlaps both ranges.*

We found that our samples could be divided in two groups: the first and larger one includes the reliefs made on models attributed to Donatello, Bartolomeo Bellano, Desiderio da Settignano and Antonio Rossellino (Virgin and Child, types of Vienna, type of the candelabra, and type of Santa Maria Nova). Works of this group were manufactured with W/P ratios over a wide range between 0.4 and 0.7. Unfortunately the small number of samples and their high dispersion prevent any finer analysis.
The two reliefs 1937-3 and Camp. 24 (both Virgin and Child, type of St Petersburg) stood apart with W/P = 0.97 and 0.88 respectively. They constitute a second group. Finally, we investigated the cast of a Virgin and Child after Luca della Robbia (Inv. 247). It exhibits a W/P of 0.80, but with individual

fragments ranging from 0.68 to 0.96, overlapping both ranges: considering this high dispersion, we did not allocate it to either group.

4.1.3 Pores morphology

The aspect ratios r_1 and r_2 of our pore data set are shown in fig. 9. They range from 0.25 to 0.40 and 0.48 to 0.60 respectively.
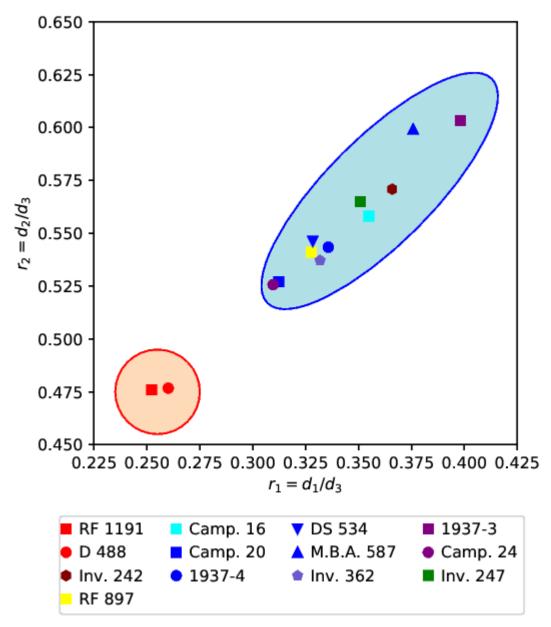

Figure 9 : averaged aspect ratios of the pores found in historic samples. *Averaged values computed from the aspect ratios of individual pores of historic samples. Reliefs of the nativity (attributed to Donatello and B. Bellano, figured in red) show low aspect ratios $r_1<0.26$ and $r_2<0.48$ compared to $0.31<r_1<0.40$ and $0.52<r_2<0.60$ for the rest of the corpus. The lower ratios indicate mesopores, and in turn hemihydrate grains, of a more elongated shape.*

Two groups can be identified: the first is constituted of reliefs D488 and RF1191, both cast on a model of the Nativity attributed to Donatello and Bartolomeo Bellano. Averaged aspect ratios of this group

were significantly lower than those of the other reliefs we sampled, gathered together in a second group.

4.2 Discussion

Even if the studied corpus of a dozen reliefs is limited (especially considering the large diffusion of these models), interesting first hypotheses can be made. The study of porosity allowed a first attempt at differentiating reliefs by crossing the information obtained through the measurement of W/P and pores morphologies. The majority of the artworks, (8 reliefs out of the 13) present common features: $0.4 <$ W/P < 0.7 and a pore shape characterised by averaged aspect ratios $0.31 < r_1 < 0.40$ and $0.52 < r_2 < 0.61$. These results support previous research led on these artworks [19,20] that report similar chemical and mineralogical composition of the plaster binder across these 8 reliefs. Moreover, all those reliefs belong to models attributed to Donatello, Desiderio da Settignano and Antonio Rossellino as they lived in Florence and suggest a certain continuity in the manufacture of 15th century Florentine reliefs.

Two pairs stand out. They differ either in the morphology of their mesopores (D488 RF119), or in their W/P ratio (1937-3, Camp 24). Both correspond to a particular model: this observation invites a more detailed discussion of each pair.

4.2.1 Nativities

According to previous [19] and ongoing studies, two reliefs D488 and RF1191 (Nativity model, the attributed to Donatello and B. Bellano) exhibit distinguishing features based on compositional and geochemical analyses. The two specimens show a W/P in line with the main group. However, the average aspect ratios of their pores are lower at $r_1 = 0.25$, 0.26 and $r_2 = 0.48$. This difference in the morphology of the pores is indicative of more elongated hemihydrate grains in the plaster powder.

This has been interpreted as a possible difference in the raw material used for plaster manufacture that can point to several possibilities. A first and most simple hypothesis is that gypsum was excavated from outcrops in the same area but showing different morphologies. The second hypothesis is that it is significative of gypsum from various sources, but supplied to the same city. Finally, they could be an indicator of the different gypsum supplies available in different cities.

Comparing the pores morphology with the center of production of these reliefs makes for an interesting case. Indeed the third relief of our corpus, cast on a model attributed to Donatello (Inv. 242, Virgin and Child, Pazzi type), falls within the main group. The attribution of the Madonna Pazzi (the marble sculpture, kept in the Bode Museum, after which relief Inv. 242 is patterned) to Florentine context is undisputed amongst art historians. The casts of the Nativity on the other hand were most likely produced in northern Italy, based on the number of reliefs of this type reported in the area [28].

The third hypothesis seems therefore likely. Additional work, including morphological as well as chemical analyses on other casts of this model, is necessary in order to reach solid conclusions.

4.2.2 Virgins and Child, type of Saint Petersburg

The two reliefs 1937-3 and Camp. 24 (Virgin and Child, type of Saint Petersburg attributed to Antonio Rossellino), show a higher W/P ratio (respectively 0.97 and 0.89), while the morphology of their pores is in line with that of the main group.

This difference in W/P indicates a difference in plaster preparation. Indeed W/P is used to control the viscosity of the plaster slurry, and the density of the set plaster (important both for weight and for mechanical properties). Two hypotheses can therefore be made to explain the higher W/P: the first one is that W/P was adjusted because of constraints in weight and durability. However all artworks in our corpus were cast in low relief, with comparable dimensions and purpose, ruling out this hypothesis. The second possibility is that W/P differs because of a different manufacturing technique. Indeed, different casting methods require slurries of different viscosity. The viscosity of the slurry can also be affected by additives, and W/P changed to compensate.

What is interesting here is that the six other reliefs, cast on four models attributed to A. Rossellino fall with the main group. Of the sampled corpus, only the two reliefs of the St. Petersburg type show a higher W/P. The difference between casts attributed to A. Rossellino could be due to an experiment with an original technique, or to craftsmen tasked with the serial manufacture of plaster casts working with different practices, either in A. Rossellino's workshop or in several Florentine ones. Ultimately it also can not be ruled out that these two casts are later imitations of 15th century reliefs.

Again, additional work with a larger corpus is required to get a better grasp of the technical variations existing in historical artworks.

5. Conclusion

We determined the water-to-plaster ratio and characterized the morphology of the reactive plaster powder for the first time on set plaster samples. These measurements were conducted on samples smaller than 1 mm^3, small enough for the characterisation of precious artworks, using synchrotron X-ray microtomography. They can give insight into both the raw material and the techniques used in the manufacture of ancient plasters.

The methodology was tested through the analysis of mock-up samples, showing consistent results in spite of the limited amount of material.

A first case study was conducted on a corpus of thirteen 15th century low-relief cast plaster sculptures. A main group of eight reliefs, all attributed to a Florentine context, was found to show similarity in both the raw material and the W/P ratio. Two casts of the Nativity, on a model attributed to Donatello and B. Bellano and most likely made in northern Italy, were differenciated by their raw material morphology. Finally, two casts of the Virgin and Child, type of St Petersburg (a model attributed to A. Rossellino) were differenciated by their higher W/P ratio. This discrepency in the casting technique could suggest variation among 15th century plaster-making practices or that the reliefs are later imitations.

These promising results show that the method introduced in this work is adequate for the investigation of ancient gypsum plasters. Its application is particularly promising for the study of Renaissance serial production of low-relief plasters, including provenance studies and the detection of possible forgeries.

References:
1) M. Oetzel, G. Heger, T. Koslowski, Einfluss von Umbegungsfeuchte und Temperatur auf die Phasenumwandlungen im System $CaSO_4$-H_2O - Ein Betrag zur Herstellung von phasenreinen Bindemitteln aus REA-Gips, ZKG Int 53:6 (2000) 354

2) H. Schmidt, I. Paschke, D. Freyer and W. Voigt, Water channel structure of bassanite at high air humidity: crystal structure of $CaSO_4$-$0.625H_2O$, Acta Crystallogr. B67 (2011) 467–475

3) S.D.M. Jacques, A. Gonzalez-Saborido, L. Leynaud, J. Bensted, M. Tyrer, R.I.W. Greaves, P. Barnes, Structural evolution during the dehydration of gypsum materials, Mineral. Mag. 73:3 (2009) 421–432

4) S. Joiret, F. Pillier, A. Lemarchand, Submicrometric Picture of Plaster Hydration: Dynamic and Space-Resolved Raman Spectroscopy versus Kinetic Monte Carlo Simulations, J. Phys. Chem. C 118 (2014) 28730−28738

5) J. Adrien, S. Meille, S. Tadier, E. Maire, L. Sasaki, In-situ X-ray tomographic monitoring of gypsum plaster setting, Cement Concrete Res. 82 (2016) 107–116

6) H. Ma, Mercury intrusion porosimetry in concrete technology: tips in measurement, pore structure parameter acquisition and application, J. Porous Mater 21. (2014) 207–215

7) K. Kovarova, R. Sevcik, Z. Weishauptova, Comparison of mercury porosimetry and X-Ray microtomography for porosimetry study of sandstones, Acta Geodyn. Geomater. 9:4 (2012) 541–549

8) D.P. Bentz, S. Mizell, et al., The visible cement data set, J. Res. Natl. Inst. Stand. 107 (2002) 137–148.

9) A. Bouterf, S. Roux, et al., Digital volume correlation applied to X-ray tomography images from spherical indentation tests on lightweight gypsum, Strain 50 (2014) 444–453

10) F. Fusseis, C. Schrank, J. Liu, A. Karrech, S. Llana-Fúnez, X. Xiao, K. Regenauer-Lieb, Pore formation during dehydration of polycrystalline gypsum observed and quantified in a time-series synchrotron radiation based X-ray micro-tomography experiment, Solid Earth 3:1 (2012) 71-86

11) J. Bedford, F. Fusseis, H. Leclère, J. Wheeler, D. Faulkner, A 4D view on the evolution of metamorphic dehydration reactions, Scientific reports, 7:1 (2017) 6881

12) A. Badde, B. Illerhaus, Three dimensional computerized microtomography in the analysis of sculpture, Scanning 30:1 (2008) 16-26

13) C. Parisi, C. Pelosi et al. The conservation project of a liturgical object : the case of Infant Jesus of Prague in the church of Saint Mary of Providence at Macchia Giarre (Italy), Eur J. Sci. Theol. 12:2 (2016) 235-234

14) A. Lee Palmer, The Walters' Madonna and Child Plaquette and Private Devotional Art in Early Renaissance Italy, J. Walters Art Mus. 59 (2001) 73-84

15) J. Pope-Hennessy, The interaction of painting and sculpture in Florence in the fifteenth century, J. Royal Soc. Arts 117 (1969) 406-424

16) G. Gentilini, Scultura dipinta o pittura a rilievo? Riflessioni sulla policromia nel quattrocento fiorentino, Techne 36 (2012) 9-17

17) G. Vasari, The lives of the artists, Oxford University Press (2008) (Translated by JC. Bondanella).

18) M. Natale, C. Ritschard, L'art d'imiter. Images de la Renaissance italienne au Musée
d'art et d'histoire, Genève : département des affaires culturelles (1997)

19) G. Gariani, P. Lehuédé., L. Leroux, G. Wallez, F. Goubard, A. Bouquillon, M. Bormand, First
insights on the mineral composition of "stucco" devotional reliefs from Italian Renaissance Masters:
investigating technological practices and raw material sourcing, J. Cult. Herit. 34 (2018) 23-32

20) A. Aksamija, W. Nowik, P. Lehuédé, M. Bormand, A. Bouquillon, Investigation of organic
additives in Italian Renaissance devotion stucco reliefs from French collections, J. Cultural Heritage
(2018), in review

21) T. Weitkamp, P. Tafforeau, E. Boller, P. Cloetens, J.-P. Valade, P. Bernard, F. Peyrin, W. Ludwig, L.
Helfen, J. Baruchel, Status and evolution of the ESRF beamline ID19, AIP Conference Proceedings
1221:1 (2010) 33-38

22) T. Weitkamp, P. Tafforeau, E. Boller, P. Cloetens, J.-P. Valade, P. Bernard, F. Peyrin, W. Ludwig, L.
Helfen, J. Baruchel, Parallel-beam imaging at the ESRF beamline ID19: current status and plans for the
future, AIP Conference Proceedings 1234:1 (2010) 83-86

23) A. Mirone, E. Gouillart, E. Bruna, P. Tafforeau, J. Kieffer, PyHST2 Hybrid distributed code for
high speed tomographic reconstruction with iterative reconstruction and a priori knowledge capabilites,
Nuclear Instrum. Methods B 324 (2014) 41–48

24) S. der Walt, J.L. Schönberger, J. Nunez-Iglesias, F. Boulogne, J.D. Warner, N. Yager, E. Gouillart,
T. Yu, Scikit-image: image processing in Python, PeerJ 2 (2014) e453

25) E. Gouillart, J. Nunez-Iglesias, S. Van Der Walt, Analyzing microtomography data with Python and
the scikit-image library, Advanced Structural and Chemical Imaging, 2:1 (2017) 18

26) N. Otsu, Threshold selection methods from gray histograms, IEEE Transactions on Systems Man
and Cybernetics 9:1 (1979) 62-66

27) C. Bezou, Étude des caractéristiques cristallographiques, thermodynamiques
et microstructurales des produits de déshydratation du gypse, PhD, Université de Bourgogne (1991)

28) C.G. Fava, La Madonna del prescepe, da Donatello a Guercino, Una devozione
antica e nuova nella terra di Cento, cat. expo, Cento, Minerva Edizioni: Pinacoteca Civita (2007) 213–
219

Images captions:
Figure 1: illustration of the two-step setting of gypsum plasters.
Figure 2: photographies of four 15th century low-relief cast sculptures, part of the corpus under study.
Figure 3: reconstructed tomography slices, showing pores and inclusions in the samples.
Figure 4: results of the measurement of W/P ratios in mock-up samples.
Figure 5: 3D visualisation of segmented pores.
Figure 6: results of the measurement of the size distributions of pores in mock-up samples.
Figure 7: results of the measurement of the morphologies of pores in mock-up samples.
Figure 8: results of the measurement of W/P ratios in historical samples.
Figure 9: results of the measurement of the morphologies of pores in historical samples.